Chinese J. Chem. Eng., **14**(6) 765—769 (2006)

Multivariable Decoupling Predictive Control Based on QFT Theory and Application in CSTR Chemical Process*

WANG Zenghui(王增会), **CHEN Zengqiang**(陈增强)**, **SUN Qinglin**(孙青林) **and YUAN Zhuzhi**(袁著祉)
Department of Automation, Nankai University, Tianjin 300071, China

Abstract A novel method of incorporating generalized predictive control (GPC) algorithms based on quantitative feedback theory (QFT) principles is proposed for solving the feedback control problem of the highly uncertain and cross-coupling plants. The quantitative feedback theory decouples the multi-input and multi-output (MIMO) plant and is also used to reduce the uncertainties of the system, stabilize the system, and achieve tracking performance of the system to a certain extent. Single-input and single-output (SISO) generalized predictive control is used to achieve performance with higher performance. In GPC, the model is identified on-line, which is based on the QFT input and the plant output signals. The simulation results show that the performance of the system is superior to the performance when only QFT is used for highly uncertain MIMO plants.
Keywords quantitative feedback theory, generalized predictive control, decouple, multivariable uncertain system, frequency domain design

1 INTRODUCTION

Many multi-input and multi-output (MIMO) systems worldwide are regarded as linear invariants, but there are still some difficulties in controlling these systems. The challenges arise from the need to achieve both robust stability and control performance when the plants to be controlled are highly uncertain[1—3]. Quantitative feedback theory (QFT) is a frequency domain design technique[4], which is perhaps the only known method that deals with highly uncertain plants[5—8] concerned with the phase information. MIMO-QFT was developed from SISO-QFT[9] and can weaken the cross-coupling between channels. The nature of QFT is quantitative; that is, the allowable closed-loop performance tolerance is quantitatively related to the level of uncertainty of the given plant[4,10]. When the condition is changed, the QFT controller must be redesigned and the tracking performance is limited to a small extent.

Generalized predictive control (GPC) is one of the long-range prediction control methods that have good robustness properties for using the future behavior of the system[11,12]. The control law is a result of minimization of the prediction output error and the incremental control values over a finite horizon. If the prediction model is identified on-line, GPC will be more robust[11,13]. At present, the GPC controller is being widely used in industrial fields[14—17].

In this study, MIMO-QFT and SISO-GPC are combined together to control highly uncertain and cross-coupling plants. MIMO-QFT is used to decouple the plants, reduce undesirable effects of variation of parameters, stabilize the system, and achieve tracking performance to some extent. SISO-GPC improves the dynamics performance of the system. The prediction models are identified depending on the MIMO-QFT input and the plant output signals. Two examples are provided to show the design procedure of the proposed technique for MIMO uncertain systems. The effectiveness of this method is shown by the simulation results.

2 BRIEF REVIEW OF MIMO-QFT

The principle of MIMO-QFT is to determine a set of MISO control systems, which are equivalent to the original system. Consider the MIMO-QFT structure shown in Fig.1.

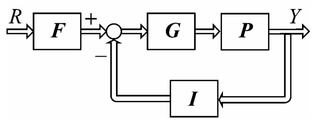

Figure 1 MIMO-QFT controller diagram

The plant transfer function matrix $\boldsymbol{P}=[p_{ij}]_{m\times m}$ is uncertain. For MIMO-QFT, $\boldsymbol{P}$ should be square and minimum-phase. If $\boldsymbol{P}$ is not square or minimum-phase, the weighting matrix is required[18,19]. Here, it is assumed that all conditions are met. $\boldsymbol{F}$ is the prefilter matrix, and $\boldsymbol{G}$ is the closed loop controller matrix.

From Fig.1, the system transfer function matrix is:

$$\boldsymbol{T}=[\boldsymbol{I}+\boldsymbol{PG}]^{-1}\boldsymbol{PGF} \tag{1}$$

For simplification, $\boldsymbol{G}$ is designed as a diagonal matrix.

Received 2005-09-20, accepted 2006-07-07.
* Supported by the National Natural Science Foundation of China (No.60374037, No.60574036), the Program for New Century Excellent Talents in Education Ministry (NCET), and the Specialized Research Fund for the Doctoral Program of Higher Education of China (No.20050055013).
** To whom correspondence should be addressed. E-mail: chenzq@nankai.edu.cn

$$G = \text{diag}[g_1, g_2, \cdots, g_m] \quad (2)$$

Premultiplying Eq.(1) by $[I+PG]$

$$[I + PG]T = PGF \quad (3)$$

Because P is nonsingular, Eq.(3) can be premultiplied:

$$[P^{-1} + G]T = GF \quad (4)$$

The matrix P^{-1} is partitioned to the form:

$$P^{-1} = \Lambda + B \quad (5)$$

where Λ is the diagonal part, and B is the balance of P^{-1}.

Using Eq.(5), Eq.(4) can be rearranged to the form:

$$T = [\Lambda + G]^{-1}[GF - BT] \quad (6)$$

The elements of matrix Q are defined as:

$$q_{ij} = \frac{\det P}{\text{adj} p_{ij}} \quad (7)$$

Thus, the elements of matrix T have the form:

$$t_{ij} = w_{ij}[v_{ij} - d_{ij}] \quad (8)$$

where $w_{ij} = \dfrac{q_{ii}}{1 + g_i q_{ii}}$, $v_{ij} = g_i f_{ij}$, and $d_{ij} = \sum_{\substack{k=1 \\ k \neq i}}^{m} \dfrac{t_{kj}}{q_{jk}}$.

Horowitz[9] has proved the fact that the MIMO system design is equivalent to the design of MISO systems. If P is a 2×2 case, there are 4 subsystems according to Eq.(8) shown in Fig.2.

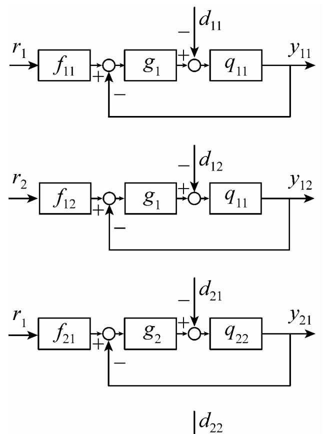

Figure 2 2×2 MIMO equivalent diagram

If d_{ij} is treated as the disturbance input, the MISO system design becomes SISO-QFT design[4]. The objective of the design is to have each loop track its desired input while minimizing the outputs because of the disturbance inputs.

3 BRIEF REVIEW OF GPC

GPC developed by Clarke *et al.*[11] is based on the CARIMA model:

$$A(z^{-1})y(t) = B(z^{-1})u(t-1) + C(z^{-1})\xi(t)/\Delta \quad (9)$$

where z^{-1} is the backward shift operator, and $A(z^{-1})$, $B(z^{-1})$, $C(z^{-1})$, and Δ are the polynomials of z^{-1}.

$$A(z^{-1}) = 1 + a_1 z^{-1} + \cdots + a_{na} z^{-na};$$

$$B(z^{-1}) = b_0 + b_1 z^{-1} + \cdots + b_{na} z^{-na};$$

$$C(z^{-1}) = 1 + c_1 z^{-1} + \cdots + c_{na} z^{-na};$$

$$\Delta = 1 - z^{-1}$$

$\{u(t)\}$, $\{y(t)\}$, and $\{\zeta(t)\}$ are the plant input, plant output, and the Gaussian white noise sequence with zero mean, respectively.

The cost function used in the GPC algorithm is:

$$J = \sum_{j=N_0}^{N_1} [y(t+j) - w(t+j)]^2 + \sum_{j=1}^{N_u} \lambda(j)[\Delta u(t+j-1)]^2 \quad (10)$$

where w is the expected output, $\lambda(j)$ is the control weight sequence, N_0 and N_1 are the minimum and maximum output prediction horizons, respectively, and N_u is the prediction control horizon. The future output and control increment can be obtained through the scroll optimizing and the feedback tuning theory based on the Diophantine equation. The following control signal can then minimize the cost function Eq.(10)[11].

$$u(t) = u(t-1) + [1, 0, \cdots, 0][H^{\mathrm{T}}H + \lambda I]^{-1} H^{\mathrm{T}}(W - F) \quad (11)$$

4 PREDICTIVE CONTROL BASED ON QFT DECOUPLING

To control the highly uncertain and cross-coupling plants, MQFT is used to decouple the plants and reduce the plant uncertainties, stabilize the systems, and achieve track performance to some extent. As GPC has some characteristics of low-pass filter, the preposition controller matrix F may not be needed. SISO-GPC controllers are used to improve the system's dynamics performance. The prediction models are identified depending on the MIMO-QFT input and the plant output. Here, recursive least square identification is used to obtain the prediction models. The control structure block diagram is shown in Fig.3. Where GPC-C_i (i=1, 2, ···, m) is the discrete-time SISO-GPC controller; c_1, c_2, ···, c_m are the SISO-GPC controllers'digital control values; ZOH is the zero-order holder; h_1, h_2, ···, h_m are the ZOH output, which are the decoupled model inputs, and the decoupled model f=PG/(I+PG), where G is the continuous-time MQFT controller matrix QFT-G; e_i=h_i−y_i (for i=1, 2, ···, m) are the QFT controller inputs.

To design the closed-loop controller G, certain specifications, such as robust stability margin, disturbance attenuation, and cross-coupling bounds, must be considered for the MIMO-QFT controller design. This MIMO-QFT controller is not limited to one or several kinds of MIMO-QFT methods; that is, various MIMO-QFT design methods can be used; sometimes the controller matrix G may not be diagonal.

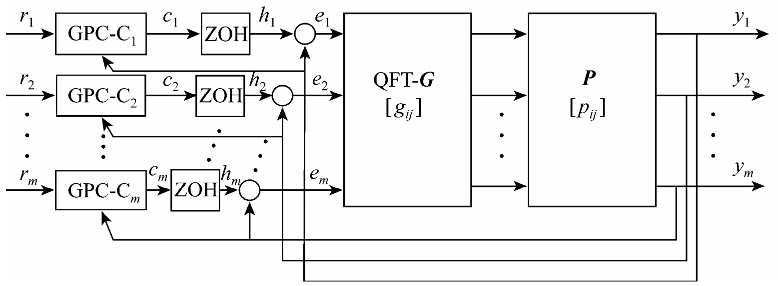

Figure 3 The control structure block diagram

In this control system, GPC is based on the identified model. The GPC controller can be designed without prior knowledge regarding the plant. Several parameters must be set according to the specifications. The control system exhibits a good performance after the controller is fitted into the system. Similar to MIMO QFT, many results of GPC can be used in this control structure. Moreover, because several SISO GPC controllers are used and self-regulated in the MIMO system, parallel computing becomes possible, which will considerably save runtime.

As mentioned above, the controller can be designed using two steps:

(1) The MIMO-QFT controller is designed according to the robust stability margin, the disturbance attenuation, the cross-coupling bounds, and so on.

(2) The GPC controller is designed for every main channel of the plant according to the control performance, for example, the tuning time.

5 SIMULATION EXAMPLES

To analyze the control efficacy of the method, two simulation examples are presented.

5.1 Example 1

The system to be controlled is a 2×2 plant with a transfer function matrix

$$\boldsymbol{P}(s)=\begin{bmatrix}\dfrac{k_{11}}{1+sA_{11}} & \dfrac{k_{12}}{1+sA_{12}}\\ \dfrac{k_{21}}{1+sA_{21}} & \dfrac{k_{22}}{1+sA_{22}}\end{bmatrix} \quad (12)$$

and a total of nine plant conditions, which are given in Table 1[9]. It is shown in Table 1 that the variation of the plant parameters is large.

Table 1 Nine plant conditions

No.	k_{11}	k_{22}	k_{12}	k_{21}	A_{11}	A_{22}	A_{12}	A_{21}
1	1	2	0.5	1	1	2	2	3
2	1	2	0.5	1	0.5	1	1	2
3	1	2	0.5	1	0.2	0.4	0.5	1
4	4	5	1	2	1	2	2	3
5	4	5	1	2	0.5	1	1	2
6	4	5	1	2	0.2	0.4	0.5	1
7	10	8	2	4	1	2	2	3
8	10	8	2	4	0.5	1	1	2
9	10	8	2	4	0.2	0.4	0.5	1

To control this plant, the MIMO-QFT controller is used and the system specifications are the same as those described in Ref.[10]. Therefore, the MIMO-QFT controller described in Ref.[10] can be used. The QFT controller matrix $\boldsymbol{G}$ is diagonal.

$$g_{11}(s)=\frac{4.1(s/1.17+1)(s/126.17+1)}{s(s/40.73+1)(s^2/360^2+s/360+1)}$$

$$g_{22}(s)=\frac{4.6(s/0.60+1)(s/45.33+1)}{s(s/10.19+1)(s^2/180^2+s/180+1)}$$

If only MIMO-QFT is used to control the plant, the prefilters used must be diagonal.

$$f_{11}(s)=\frac{1}{(s/2.5+1)} \quad \text{and} \quad f_{22}(s)=\frac{1}{(s/2.0+1)}$$

If the expected outputs are square wave signals within the ranges [−5, 5] and [−2.5, 2.5], respectively, the time responses y_1 and y_2 with respect to the nine plant conditions are as shown in Fig.4.

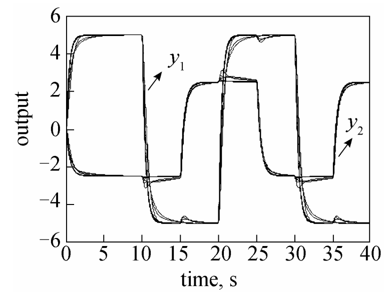

Figure 4 The response of only MIMO-QFT controller

If no prefilter controller is used, time responses of the system with respect to the nine plant conditions are as shown in Fig.5.

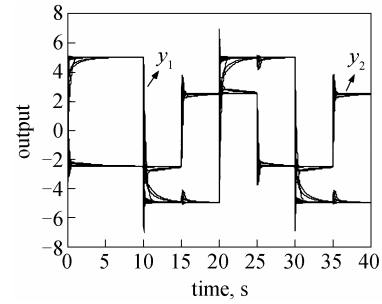

Figure 5 The response of only QFT controller without prefilter

If the GPC controller used is based on MIMO-QFT decoupling, the time responses of the system with respect to the nine plant conditions are as shown in Fig.6. The GPC parameters are designed as: $n_a = 2$, $n_b = 1$, $N_0 = 0$, $N_1 = 6$, $N_u = 3$, $\lambda = 0.2$, $C(z^{-1}) = 1$, and the softening factor α=0.8.

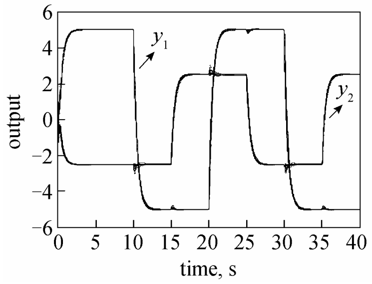

Figure 6 The response of predictive control based on MIMO-QFT decoupling

5.2 Example 2

A nonisothermal CSTR with large parametric uncertainty is controlled. The CSTR model is a MIMO linear state space model obtained for the reactor data around the steady state [20].

$$\begin{cases} \boldsymbol{x} = \boldsymbol{A}_{\text{cstr}}\boldsymbol{x} + \boldsymbol{B}_{\text{cstr}}\boldsymbol{u} \\ \boldsymbol{y} = \boldsymbol{C}_{\text{cstr}}\boldsymbol{x} \end{cases}$$

where

$$\boldsymbol{A}_{\text{cstr}} = \begin{bmatrix} a_{11} & -41.11 & 0 \\ -0.00386 & a_{22} & 0 \\ 2 & 20.5 & -1 \end{bmatrix},$$

$$\boldsymbol{B}_{\text{cstr}} = \begin{bmatrix} b_{11} & 0 \\ 0.1304 & b_{22} \\ 1 & 0 \end{bmatrix}, \quad \boldsymbol{C}_{\text{cstr}} = \begin{bmatrix} 1 & 0 & 0 \\ 0 & 1 & 0 \end{bmatrix}$$

The elements a_{11}, a_{22} b_{11}, and b_{22} experience uncertainty as given below:

$$a_{11} \in [-8, -3], a_{22} \in [-3, -0.75],$$
$$b_{11} \in [-4, -15], b_{22} \in [-0.05, -0.01].$$

If the controllers are the same as those described in Ref.[20], the following equations are obtained

$$\boldsymbol{G}(s) = \begin{bmatrix} \dfrac{-5\times10^4(s/5+1)(s/100+1)}{s(s/8+1)(s/2000+1)} & 0 \\ 0 & \dfrac{-4\times10^4(s/6+1)}{(s/0.8+1)(s/60+1)} \end{bmatrix},$$

$$\boldsymbol{F}(s) = \begin{bmatrix} \dfrac{1}{(s/5+1)(s/10+1)} & 0 \\ 0 & \dfrac{1}{(s/6.5+1)^2} \end{bmatrix},$$

and the responses of the systems are shown in Fig.7 for the four conditions listed in Table 2.

As GPC can only deal with low frequencies, and the response time of this system is considerably less, low-pass filters are needed for GPC controllers. If the GPC controller and the low-pass filters are used, which are based on MIMO-QFT decoupling, the response time of the system with respect to the four plant conditions are as shown in Fig.8. The GPC parameters are designed as: $n_a = 4$, $n_b = 3$, $N_0 = 0$, $N_1 = 4$, $N_u = 2$, $\lambda = 0.2$, $C(z^{-1}) = 1$, and the softening factor α=0.7.

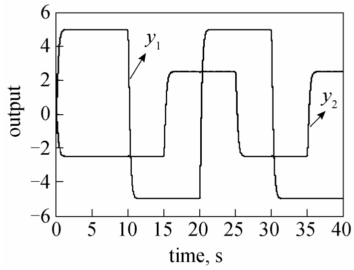

Figure 7 The response of only MIMO-QFT controller

Table 2 Four plant conditions

No.	a_{11}	a_{22}	b_{11}	b_{22}
1	−6	−3	−4	−0.05
2	−5	−2	−3	−0.04
3	−4	−1	−2	−0.02
4	−3	−0.75	−1.5	−0.01

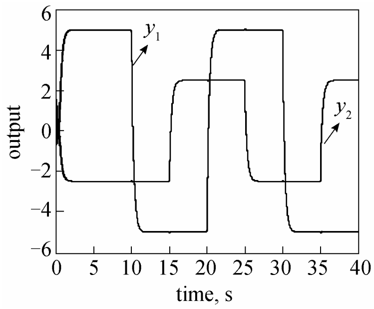

Figure 8 The response of the predictive control based on MIMO-QFT decoupling

Here, the low-pass filters transfer function is chosen as:

$$f_{\text{low}}(s) = \frac{1}{s/10+1}$$

The system shows a steady error of about 0.01 when the output lines y_2 in Fig.7 are magnified. This is because the controller does not include the integral section. As GPC has an integral effect, there is no steady error in Fig.8, and the proposed method can easily change the tracking performance. It is clear that the proposed approach can provide better control performance than that obtained when only single MIMO-QFT controllers are used.

6 CONCLUSIONS

In this article, a predictive controller based on MIMO-QFT is proposed. This method can utilize

MIMO-QFT effectively to decouple and control the plant. The tracking performance can be easily adjusted through the soften factor of GPC. Several SISO GPC controllers can be computed in parallel for saving the runtime. The simulation examples demonstrate the effectiveness of this technique.

NOMENCLATURE

A	polynomial of output of the system model
$\boldsymbol{A}_{\mathrm{cstr}}$	system state matrix
$\boldsymbol{A}_{ij}$	parameters of the transfer function matrix
a_i	coefficients of $\boldsymbol{A}$
B	polynomial of input of the system model
$\boldsymbol{B}$	balance of $\boldsymbol{P}^{-1}$
$\boldsymbol{B}_{\mathrm{cstr}}$	system input matrix
b_i	coefficients of $\boldsymbol{B}$
C	polynomial of disturbance of the system model
$\boldsymbol{C}_{\mathrm{cstr}}$	system output matrix
c_i	coefficients of $\boldsymbol{C}$
$\boldsymbol{F}$	prefilter matrix
f_{ij}	element of $\boldsymbol{F}$
$\boldsymbol{G}$	closed loop controller matrix
g_{ij}	elements of $\boldsymbol{G}$
$\boldsymbol{H}$	step response matrix
$\boldsymbol{I}$	unit matrix
J	cost function of GPC
k_{ij}	parameters of the transfer function matrix
N_u	control horizon
N_0	minimum output horizon
N_1	maximum output horizon
n_{a}	degree of $\boldsymbol{A}$
n_b	degree of $\boldsymbol{B}$
n_c	degree of $\boldsymbol{C}$
$\boldsymbol{P}$	transfer function matrix of the uncertain plant
p_{ij}	element of $\boldsymbol{P}$
s	Laplace operator
$\boldsymbol{T}$	systems transfer function matrix
t_{ij}	element of $\boldsymbol{T}$
u	control variable of the system
$\boldsymbol{u}$	system control vector
$\boldsymbol{W}$	future set-point vector
w	element of $\boldsymbol{W}$
$\boldsymbol{x}$	system state vector
y	output variable of the system
$\boldsymbol{y}$	system output vector
z^{-1}	backward shift operator
α	soften factor ($0<\alpha<1$)
Δ	symbol of backward difference
ζ	white noise sequence with zero mean
$\boldsymbol{\Lambda}$	diagonal matrix
λ	control weight factor ($\lambda>0$)

Subscripts

i	index of variables
j	index of variables

REFERENCES

1 Zhang, L., He, X.R., Xu, Q., "Modified model for flexibility analysis in chemical engineering processes", *Chin. J. Chem. Eng.*, **12**(5), 673—676(2004).

2 Zhou, L.F., Qian, J.X., "The IMC structure of multi-rate multivariable predictive control systems and an improved algorithm", *Chin. J. Chem. Eng.*, **9**(3), 273—279(2001).

3 Zhang, L., He, X.R., Xu, Q., "A modified model for flexibility analysis in chemical engineering processes", *Chin. J. Chem. Eng.*, **12**(5), 673—676(2004).

4 Horowitz, I., "Survey of quantitative feedback theory (QFT)", *Int. J. Control*, **53**(2), 255—291(1991).

5 Wu, S.F., Grimble, M.J., Wei, W., "QFT-based robust/fault-tolerant flight control design for remote pilotless vehicle", *IEEE Trans. Contr. Syst. Technol.*, **8,** 1010—1016(2000).

6 Karpenko, M., Sepehri, N., "Fault-tolerant control of a servohydraulic positioning system with crossport leakage", *IEEE Trans. Contr. Syst. Technol.*, **13**, 155—161(2005).

7 Pachter, M., Houpis, C.H., Kang, K., "Modeling and control of an electro-hydrostatic actuator", *Int. J. Robust Nonlinear Control*, **7**, 591—608(1997).

8 Niksefat, N., Sepehri, N., "A QFT fault-tolerant control for electrohydraulic positioning systems", *IEEE Trans. Contr. Syst. Technol.*, **10,** 626—632(2002).

9 Horowitz, I., "Quantitative synthesis of uncertain multiple input-output feedback system", *Int. J. Control*, **30**(1), 81—106(1979).

10 Cheng, C.C., Liao, Y.K., Wang, T.S., "Quantitative feedback design of uncertain multivariable control system", *Int. J. Control*, **65**(3), 537—553(1996).

11 Clarke, D.W., Mohtadi, C., Tuffs, P.S., "Generalized predictive control: Part 1 and Part 2", *Automatica*, **23**(1), 137—160(1987).

12 Richalet, J., Rault, A., Testud, J.L., Papon, J., "Model predictive heuristic control: Applications to industrial processes, *Automatica*, **14**(5), 413—428(1978).

13 Demircioglu, H., Karasu, E., "Generalized predictive control–A practical application and comparison of discrete- and continuous-time versions", *IEEE Contr. Syst. Mag.*, **20**(5), 36—47(2000).

14 Yu, S.M., Wang, H.Q., "Improved generalized predictive control algorithm with offline and online identification and its application to fixed bed reactor", *Chin. J. Chem. Eng.*, **11**(1), 49—54(2003).

15 Grimble, M.J., Ordys, A.W., "Predictive control for industrial applications", *Annu. Rev. Control*, **25**, 13—24(2001).

16 Chen, Z.Q., Mao, Z.X., Du, S.Z., Sun, Q.L., Yuan, Z.Z., "Analysis of robustness of PID-GPC based on IMC structure", *Chin. J. Chem. Eng.*, **11**(1), 55—61(2003).

17 Sun, Q.L., Chen, Z.Q., Yuan, Z.Z., Liu, Z.X., Yang, X.J., "β-GPC control system of heat treatment for welded drill pipe", *Control Theory Appl.*, **19**(6), 957—959(2002).

18 Houpis, C.H., Sating, R.R., "MIMO QFT CAD pachage (Version 3)", *Int. J. Robust Nonlinear Control*, **7,** 533—549(1997).

19 Houpis, C.H., Sating, R.R., Rasmussen, S., Sheldon, S., "Quantitative feedback theory technique and applications", *Int. J. Control*, **59**(1), 39—70(1994).

20 Patel, H.J., Nataraj, P.S.V., "Robust multivariable feedback design for an uncertain non-isothermal CSTR", In: Proceedings of the 32nd Conference on Decision and Control, San Antonio, Texas, 3871—3876(1993).